Available online at www.sciencedirect.com

ScienceDirect

Physics Procedia 56 (2014) 1325 – 1333

Physics Procedia

8th International Conference on Photonic Technologies LANE 2014

Finite-difference time-domain modeling of laser-induced periodic surface structures

G.R.B.E. Römer[a,*], J.Z.P. Skolski[a,b], J. Vincenc Oboňa[a,b], A.J. Huis in 't Veld[a]

[a] *University of Twente, Chair of Applied Laser Technology, Drienerlolaan 5, Enschede, 7522NB, The Netherlands*
[b] *M2i Materials innovation institute, Mekelweg 2, 2628CD, Delft, The Netherlands*

Abstract

Laser-induced periodic surface structures (LIPSSs) consist of regular wavy surface structures with amplitudes the (sub)micrometer range and periodicities in the (sub)wavelength range. It is thought that periodically modulated absorbed laser energy is initiating the growth of LIPSSs. The "Sipe theory" (or "Efficacy factor theory") provides an analytical model of the interaction of laser radiation with a rough surface of the material, predicting modulated absorption just below the surface of the material. To address some limitations of this model, the finite-difference time-domain (FDTD) method was employed to numerically solve the two coupled Maxwell's curl equations, for linear, isotropic, dispersive materials with no magnetic losses. It was found that the numerical model predicts the periodicity and orientation of various types of LIPSSs which might occur on the surface of the material sample. However, it should be noted that the numerical FDTD model predicts the signature or "fingerprints" of several types of LIPSSs, at different depths, based on the inhomogeneously absorbed laser energy at those depths. Whether these types of (combinations of) LIPSSs will actually form on a material will also depend on other physical phenomena, such as the excitation of the material, as well as thermal-mechanical phenomena, such as the state and transport of the material.

Peer-review under responsibility of the Bayerisches Laserzentrum GmbH

Keywords: Laser-induced Periodic Surface Structures; Model; LIPSS; Maxwell curl equations; FDTD

1. Introduction

Laser-induced periodic surface structures (LIPSSs) are periodic wavy surface features, or *ripples*, observed on many types of materials, including semiconductors (Birnbaum, 1965; Emmony et al., 1973; Young et al., 1983), metals (Siegrist, 1973; Jee et. al., 1988), dielectrics (Temple and Soilau, 1981) and polymers (Baudach et al., 1999; Csete et al., 2004). The LIPSSs are usually categorized, based on the spatial periodicity Λ, see Table 1 for an overview. First, when the spatial periodicity Λ of the LIPSSs is usually close to the laser wavelength λ and the LIPSS are oriented orthogonal to the polarization of the light, the LIPSSs are commonly referred to as *Low Spatial Frequency LIPSSs* (LSFLs), but also as *regular ripples* (Römer et al., 2009). LSFLs can be formed by continuous wave (cw), as well as pulsed laser radiation. However, for ultra-short laser pulses, the periodicity of LSFLs may be smaller than the laser

* Corresponding author. Tel.: +31-53-4892519 ; fax: +31-53-4893631 .
E-mail address: g.r.b.e.romer@utwente.nl

Peer-review under responsibility of the Bayerisches Laserzentrum GmbH
doi:10.1016/j.phpro.2014.08.058

Table 1. Spatial periodicity Λ of LIPSSs–i.e. of LSFL and HSFL, compared to the wavelength λ of the laser radiation for various materials. LSFL are oriented orthogonal to polarisation direction of the laser radiation. HSFL can both be oriented orthogonal ($\perp$) or parallel ($\parallel$) to the polarisation. In the referenced articles, the LIPSSs were produced at normal incidence of the laser beam.

Material	Type	Periodicity Λ	Source
Si	LSFL	$\Lambda \approx 0.94\lambda$	Haneman and Nemanich (1982)
Si	LSFL	$0.7 \leq \Lambda/\lambda \leq 0.96$	Costache et al. (2004); Bonse et al. (2002, 2009, 2010)
Si	HSFL,$\parallel$	$\Lambda \approx 0.25\lambda$	Costache et al. (2004)
Molten quartz	LSFL	$\Lambda \approx 0.71\lambda$	Keilmann and Bai (1982)
NaCl	LSFL	$\Lambda \approx 0.67\lambda$	Temple and Soilau (1981)
Ti	HSFL, $\parallel$	$0.08 \leq \Lambda/\lambda \leq 0.12$	Bonse et al. (2013)
TiN	LSFL	$\Lambda \approx 0.74\lambda$	Bonse et al. (2000)
TiN	HSFL, $\perp$	$\Lambda \approx 0.16$	Yasumaru et al. (2003)
Alloyed steel (800H)	LSFL	$\Lambda \approx 0.63\lambda$	Huis in 't Veld and van der Veer (2010)
Alloyed steel (800H)	HSFL, $\parallel$	$0.15 \leq \Lambda/\lambda \leq 0.24$	Huis in 't Veld and van der Veer (2010)
Pt	LSFL	$0.66 \leq \Lambda/\lambda \leq 0.76$	Vorobyev et al. (2007)
InP	LSFL	$0.74 \leq \Lambda/\lambda \leq 0.94$	Bonse et al. (2005)
InP	HSFL, $\perp$	$\Lambda \approx 0.24\lambda$	Borowiec and Haugen (2003)
Diamond	LSFL	$\Lambda \approx 0.94\lambda$	Wu et al. (2003)
Diamond	HSFL, $\parallel$	$\Lambda \approx 0.26\lambda$	Wu et al. (2003)
ZnO	HSFL, $\perp$	$0.25 \leq \Lambda/\lambda \leq 0.35$	Borowiec and Haugen (2003)
Sapphire	HSFL, $\perp$	$\Lambda \approx 0.34\lambda$	Borowiec and Haugen (2003)

wavelength. In any case, LSFLs mainly form at fluence levels close to the single pulse ablation threshold. The second type of LIPSSs show a periodicity (much) smaller than the laser wavelength–i.e. $\Lambda \ll \lambda$, and are usually referred to as *High Spatial Frequency LIPSSs* (HSFLs), but also as *fine ripples* (Okada et al., 2008; Römer et al., 2009). HSFLs are formed on the surface when ultra-short laser pulses, with durations in the femtosecond and picosecond regime, are applied. The third type of LIPSSs form when the surface is exposed to high pulse energy and/or numerous pulses–i.e. when the surface is exposed to a high energy dose. These LIPSSs exhibit a spatial periodicity larger than the laser wavelength–i.e. $\Lambda > \lambda$, and are usually referred to as *Grooves*. The Grooves usually occur on locations on the surface where a significant ammount of material has been removed. The preferential orientation of Grooves is usually parallel to the polarization direction of the laser radiation (Skolski et al., 2013; Bonse et al., 2010, 2005), but in rare cases can be orthogonal to the polarization (Huang et al., 2010).

The spatial periodicity, orientation and amplitude of these LIPSSs vary with the number of laser pulses applied (Skolski, 2014), as well as with the angle of incidence of the laser beam with the surface (Young et al., 1983). When exposing the material to circularly polarized laser radiation (at normal incidence), no well-defined ripples are formed, but cone-like protrusions or holes form, which are isotropically speckled on the surface (van Driel, 1982; Camacho-López et al., 2012).

This paper discusses (the results of) a numerical model, aimed at the prediction of the periodicity and orientation of LSFL, HSFL and Grooves. This model includes a qualitative description of material removal (ablation) in order to verify whether this phenomenon can explain the growth of Grooves. Usually, simulation results are presented and discussed in the frequency domain. However, this paper presents and discusses the results in the space domain.

2. Model

2.1. Efficacy factor theory

The strong correlation of the periodicity of LIPSSs to the laser wavelength, as well as the strong correlation of the orientation of LIPSSs to the polarization, suggest that their formation, or at least the early stages of LIPSSs formation (Höhm et al., 2013; Derrien et al., 2013), can be explained by an electromagnetic approach. That is, LIPSSs formation is explained as the result of the interaction of laser radiation, with the rough surface of the material.

The theory of Sipe et al. (1983), which is also referred to as "Sipe's theory" or *Efficacy factor theory*, provides a mathematical description of this interaction. This theory predicts that the absorbed laser energy, just below the surface, shows a spatial periodicity. Moreover, it is assumed that LIPSSs originate at the locations where the level of

absorbed energy is the largest. Mathematically, Sipe's theory is defined in the frequency domain and states that the inhomogeneous energy absorption $A(\vec{k})$ is proportional to

$$A(\vec{k}) \propto \eta(\vec{k}, \vec{k}_i)|b(\vec{k})|\,, \tag{1}$$

where $\vec{k} = (k_x, k_y)$ is a vector spanning the frequency domain parallel to the surface and normalized by the norm of the wave vector $\vec{k}$. Further, $b(\vec{k})$ is the Fourier transform of the surface roughness. Here, $\eta(\vec{k}, \vec{k}_i)$ is the *Efficacy factor* determining efficiency by which the surface roughness $b(\vec{k})$ leads to an inhomogeneous energy absorption at frequency component $\vec{k}$. Based on these definitions, Sipe et al. (1983) describe the procedure to derive an analytical expression for $\eta(\vec{k}, \vec{k}_i)$ given the statistical properties of the surface roughness (in terms of a *filling factor* and a *shape factor*), laser wavelength, angle of incidence and the optical properties (complex index of refraction $\tilde{n}$) of the material under consideration.

Unfortunately the Efficacy factor theory suffers from some limitations, when trying to predict, for example, some properties of HSFLs and Grooves. These limitations can be attributed to the fact that, to calculate $\eta(\vec{k}, \vec{k}_i)$, the Efficacy factor theory assumes that:

1. the optical properties of the material (complex index of refraction $\tilde{n}$) are constant, despite the fact that the optical properties of the material change significantly during the laser pulse,
2. the amplitude of the surface roughness is (much) smaller than the wavelength λ of the incident laser radiation. As this assumption may be valid for the initial roughness of the surface, it will definitely not be the case in multi pulse experiments, when LIPSSs with large(r) amplitudes form and grow, pulse-by-pulse (see section 3),
3. the amplitude of the surface roughness is (much) smaller than the periodicity Λ of the inhomogeneously absorbed laser energy.

Especially the last two assumptions limit the applicability of the model to predict Grooves, because Grooves typically show a periodicity larger than the laser wavelength. Further, as $\eta(\vec{k}, \vec{k}_i)$ is computed just below the surface only, no analysis of the energy absorption in the bulk of the material is possible. Finally, the model does not allow to calculate the shape and dimensions (amplitude) of the absorbed laser energy in the spatial domain, but only in the frequency domain.

2.2. Finite-difference time-domain model

To address some of the limitations addressed above, we employed the finite-difference time-domain (FDTD) method (Yee, 1966) to numerically solve the two coupled Maxwell's curl equations, for linear, isotropic, dispersive materials with no magnetic losses, in the 3D space and time domain (Skolski et al., 2012; Skolski, 2014)

$$\mu_0 \frac{\partial \vec{H}}{\partial t} = -\vec{\nabla} \times \vec{E} \quad \text{and} \quad \epsilon_0 \epsilon_r \frac{\partial \vec{E}}{\partial t} + \sigma \vec{E} = -\vec{\nabla} \times \vec{H}\,, \tag{2}$$

where $\vec{E}$ denotes the electric field, $\vec{H}$ the magnetic field, t time, μ_0 the permeability in vacuum, ϵ_0 the permitivity in vacuum, ϵ_r the relative permitivity of the material, σ the electric conductivity of the material. To account for the changing optical properties, due to the excited state of the material as a result of absorbed laser energy, the so-called Sipe-Drude model, as proposed by (Bonse et al., 2009), was adopted. This model assumes a modified, yet still constant, complex permittivity $\tilde{\epsilon}_r^* = \tilde{\epsilon}_r + \Delta\tilde{\epsilon}_{\text{Drude}}$ of the material, by describing the transient dielectric function of the laser-excited material by a Drude model. The locally absorbed energy was computed from the sum of the electric losses $\sigma(\vec{E})^2 + \vec{J} \cdot \vec{E}$ in each cell of the numerical grid at each time step, where $\vec{J}$ denotes the Drude internal current (Skolski, 2014). It was verified that the numerical results are in good agreement with the analytical results of the Sipe-Drude model (Skolski et al., 2012; Skolski, 2014).

It was found that the FDTD model predicts the periodicity and orientation of many types of LIPSSs which might occur on the surface of a sample (Skolski, 2014; Römer et al., 2014). The FDTD simulations even indicated HSFLs oriented perpendicular to the polarization, which is not handled correctly by the analytical model of Sipe et al. However, it should be noted that the numerical FDTD model predicts the signature or "fingerprints" of several types of

LIPSSs, but whether these LIPSSs will actually form on a material will also depend on other physical phenomena. In addition, no signature of Grooves was found by using this FDTD model. This is discussed in the next subsection.

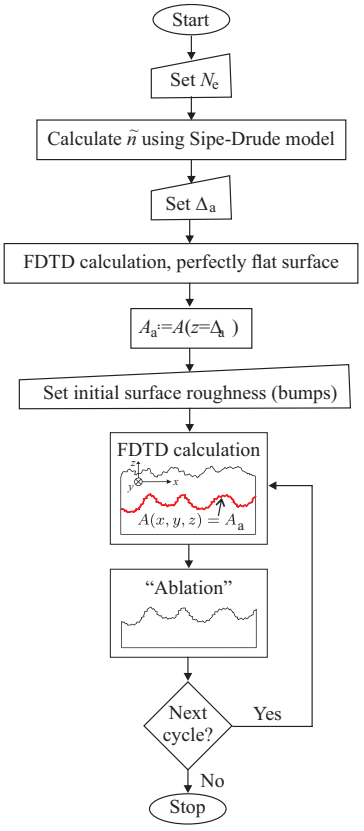

Fig. 1. Flowchart of numerical simulations including "ablation".

2.3. *Qualitative ablation model*

Besides the absorbed laser energy, LIPSS formation is also affected by other physical phenomena occurring during and/or after the laser pulse, such as, but not limited to, free electron generation, electron heating, electron-phonon coupling, non-thermal melting, (in)homogeneous melting and ablation mechanisms like spallation, hetero- & homogeneous nucleation (phase explosion), and fragmentation (Rethfeld et al., 2004; Breitling et al., 2004; Lorazo et al., 2006; Zhigilei et al., 2009; Perez and Lewis, 2003; Lewis and Perez, 2009). To compute the effects of these phenomena would require a Two-Temperature Model (TTM) in order to model the distribution and diffusion of absorbed energy in the electron gas, and the energy transfer to the lattice, as well as numerous additional models to account for material excitation, transport and ablation, mentioned above. Analyse these effects numerically, computational demanding techniques, such as Gas Dynamics, Molecular Dynamics and Monte Carlo would be required (Leveugle et al., 2004; Anisimov et al., 2008; Lorazo et al., 2006; Zhigilei et al., 2009; Perez and Lewis, 2003; Lewis and Perez, 2009). Moreover, the FDTD model, described in the previous subsection, allows to compute the absorbed laser energy in the substrate due to a one plane wave only. The properties of LIPSSs are known to vary on a pulse-to-pulse basis, as every subsequent laser pulse is "confronted" with the LIPSSs formed by the previous laser pulse.

In order to quickly evaluate whether Grooves formation could be explained on the basis of this pulse-to-pulse evolution of the surface, a simple and qualitative ablation model was incorporated into the FDTD model (Skolski, 2014). That is, once the absorbed laser energy $A(x, y, z)$ is computed by an FDTD simulation, the plane (x, y, z) of

a constant absorptivity A_a is determined. Here, A_a denotes the absorbed energy threshold at which ablation of the material occurs. Next, the material above the plane is removed ("ablated") from the simulation domain, resulting in a new/updated surface roughness due to the "pulse" under consideration. This updated surface topography is fed into the next run of the FDTD simulations (referred to as an FDTD *cycle*), resulting in a new absorbed energy profile in the material, see Fig. 1. This iteration of simulations (FDTD cycles) is repeated until the surface profile converges.

The absorbed energy threshold A_a is related to an ablation depth Δ_a below a flat surface. The latter is an input parameter of the model. Therefore, the simulations start by a FDTD run in which the initial surface is perfectly flat and the absorbed energy at the depth of Δ_a is determined. The value found is set equal to A_a.

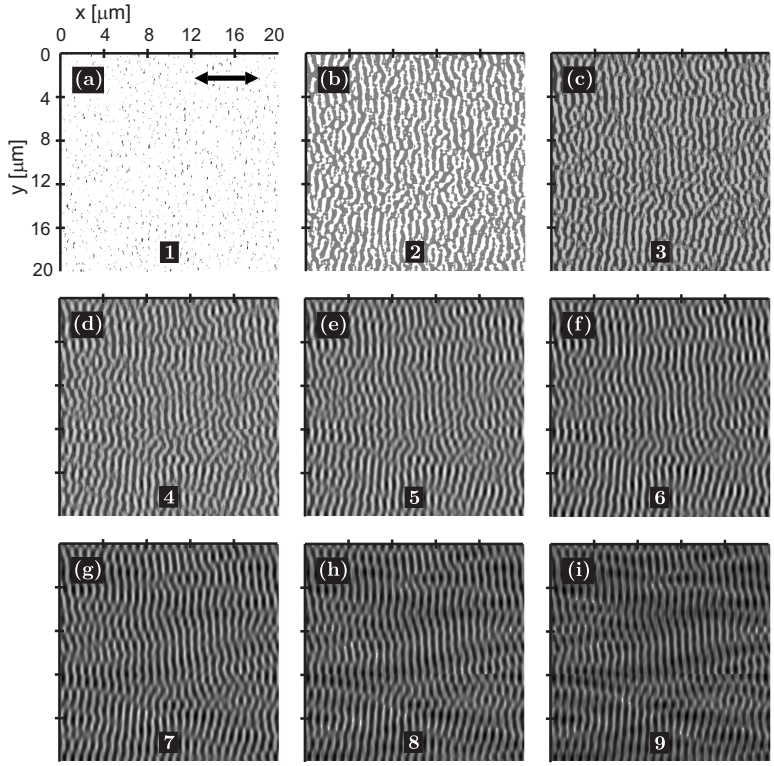

Fig. 2. Top view of the "growth" of LSFLs as function of FDTD simulation cycles, starting from an initial random rough surface. The black arrow in graph (a) indicates the polarization direction of the laser radiation. The number of FDTD cycles is indicated in the bottom of each graph. The simulations were performed with $\Delta_a = 50$nm and a complex index of refraction of $= 1.339 + 3.22\,j$, corresponding to a density of free electrons in the conduction band of silicon of $N_e = 8 \cdot 10^{27} m^{-3}$. In these graphs, peaks of the LSFL are indicated in the bright(er) scales of gray, whereas the darker grays indicate the valleys of the LSFL.

3. Simulation results

As an initial rough surface, "bumps" with heights small compared to the laser wavelength and randomly distributed over the surface, were assumed. The dimensions of the Yee cells, the 3D grid on which the Maxwell equations are numerically solved, were set to 20nm in both x and y direction, and 5nm in z direction. The time step during the simulations was set to $1.5 \cdot 10^{-17}$s. The laser radiation was modeled as a plane wave of wavelength $\lambda = 800$nm (common for femtosecond pulsed laser sources), linearly polarized along the x-axis at normal incidence to the surface, and traveling in the z-driection. The optical properties were set to those of (excited) silicon, characterized by the density of free electrons N_e and resulting complex index of refraction $\tilde{n}$, based on the above mentioned Sipe-Drude model.

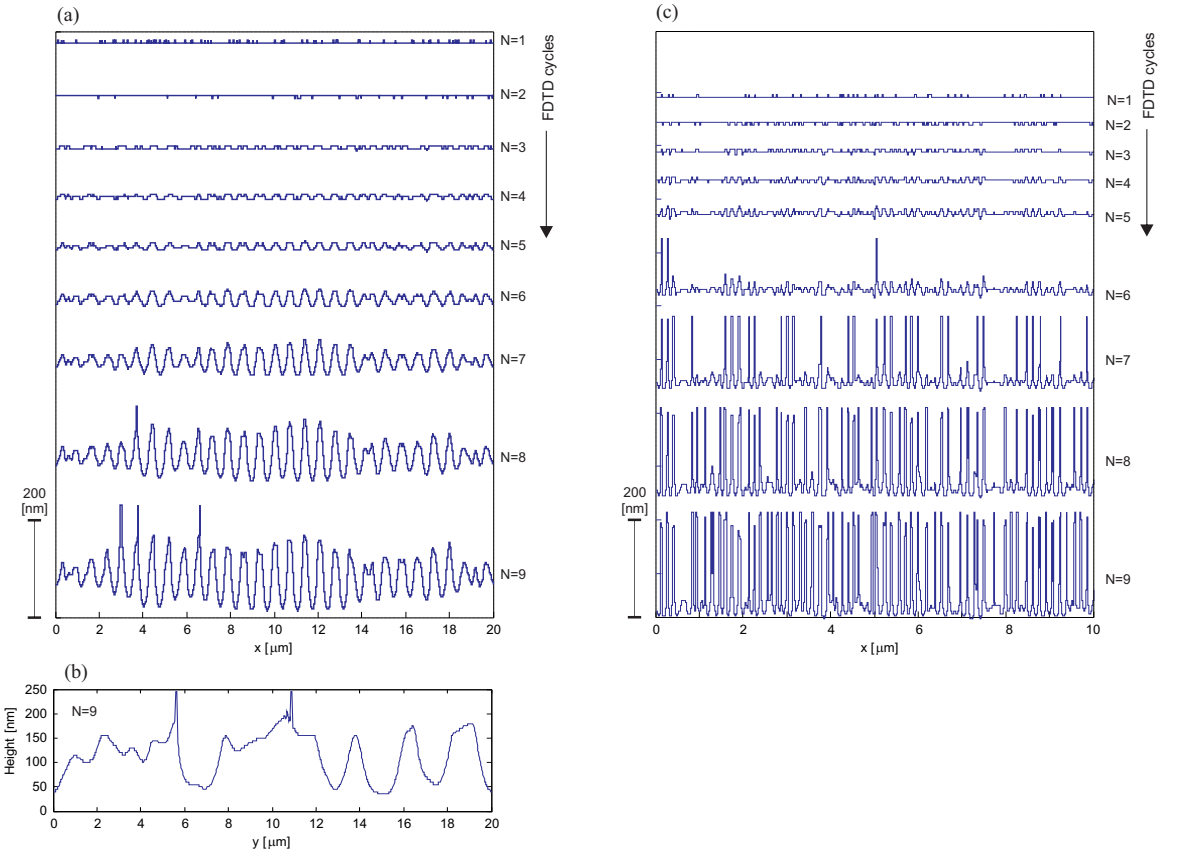

Fig. 3. Cross-sections and longitudinal section of LIPSS. (a) Cross sections of LSFL in Fig. 2 at $y = 10\mu$m, as function of the number of FDTD cycles. (b) longitudinal section of LSFL and Grooves in Fig. 2(i) at $x = 10\mu$m. (c) Cross sections of HSFL in Fig. 4 at $y = 10\mu$m, as function of the number of FDTD cycles.

3.1. Low Spatial Frequency LIPSS (LSFL) and Grooves

Fig. 2 shows a top view of the formation of LSFLs on a simulation area of $20{\times}20\,\mu\text{m}^2$, starting from the initial rough surface, as a function of the number of FDTD-feedback cycles. The FDTD feedback simulations were performed at $N_e = 8 \cdot 10^{27}\text{m}^{-3}$ (implying $\tilde{n} = 1.339 + 3.22\,j$) and $\Delta_a = 50$nm.

As can be observed from this figure, the surface morphology changes mainly during the first 3 FDTD cycles. That is, already after a first simulation run, the initial roughness is "erased" and periodic structures can be observed, see Fig. 2(b). After 9 cycles, these periodic structures are well developed, see Fig. 2(i). With increasing FDTD cycle, the structures become more regular and more oriented perpendicular to the polarization direction of the laser radiation. Fig. 3(a) shows cross sections along the x-axis (at $y = 10\mu$m) of the results in Fig. 2.

Also from this figure, it can be concluded that the periodic structures grow and become more regular with increasing FDTD cycle. The spatial periodicity of the structures in Fig. 2(i) and Fig. 3(a, bottom) was determined to be $\Lambda \approx 750$nm. It can be concluded from this periodicity, being close to the wavelength $\lambda = 800$nm of the laser, and oriented perpendicular to its polarization direction, that these periodic structures are LSFL, see Table 1. The averaged peak-to-valley height of the LSFL in Fig. 2(i) was found to equal about 125nm. Therefore, although an (over)simplified ablation model was employed, the predicted height of LSFLs are in the range of heights of LSFLs found in experiments (Oboňa et al., 2014). Hence, the FDTD model including a simplified model of ablation, predicts the formation and growth of LSFL.

Besides LSFLs, carefull analysis of Fig. 2(i) reveals a periodic structure, superimposed on the LSFLs, but oriented parallel to polarization direction. The spatial periodicity of the latter structures is larger than the wavelength of the laser. Fig. 3(b) shows the longitudinal section along the y-axis (at $x = 10\mu$m) of the results in Fig. 2(i). The spatial periodicity of these structures was found to range from 1.5μm to 3.3μm. It can be concluded from this periodicity, being larger than the laser wavelength, and oriented parallel to its polarization direction, that these periodic structures match the characteristics of Grooves. Hence, the FDTD model including the simplified model of ablation, also seems to be able to predict the formation and growth of Grooves.

3.2. High Spatial Frequency LIPSS (HSFL)

Fig. 4 shows a top view of the formation of HSFLs starting from the initial rough surface, as a function of the number of FDTD-feedback cycles. The simulation domain covered an area of $20{\times}20\ \mu\text{m}^2$, but for clarity only an area of $10{\times}10\ \mu\text{m}^2$ is shown in the figure. The FDTD feedback simulations were performed at $N_e = 4 \cdot 10^{27}\text{m}^{-3}$ (implying $\tilde{n} = 1.943 + 1.116\,j$) and $\Delta_a = 30$nm. These latter two values are smaller than in the previous subsection, where results for LSFL were shown. That is, because HSFL occur at lower laser fluence levels than LSFL, implying lower excitation of the silicon (smaller value of N_e) and smaller ablation depth, as well. Like in the previous subsection, the

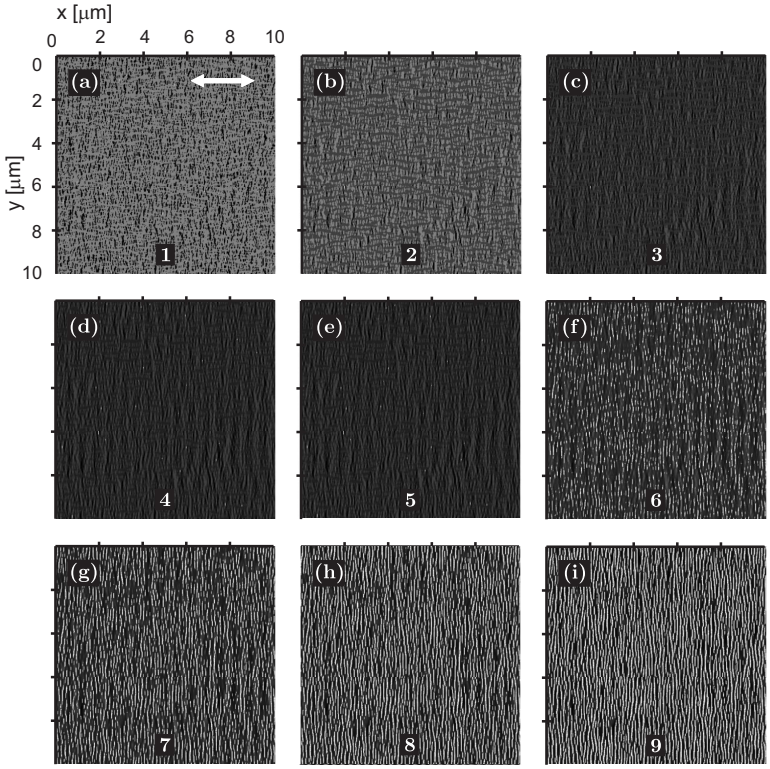

Fig. 4. Top view of the "growth" of HSFLs as function of FDTD simulation cycles, starting from an initial random rough surface. The white arrow in this graph indicates the polarization direction of the laser radiation. The number of FDTD cycles is indicated in the bottom of each graph. The simulations were performed with $\Delta_a = 30$nm and a complex index of refraction of $\tilde{n} = 1.943 + 1.116\,j$, corresponding to a density of free electrons in the conduction band silicon of $N_e = 4 \cdot 10^{27} m^{-3}$. In these graphs, peaks of the HSFLs are indicated in the bright(er) scales of gray, whereas the dark(er) grays indicate the valleys of the HSLFs.

surface morphology changes mainly during the first 3 FDTD cycles. That is, already after one or two FDTD cycles, the initial roughness is "erased" and periodic structures can be observed, see Fig. 4(c). After 9 cycles, these periodic structures are well developed, see Fig. 4(i). With increasing FDTD cycle, the structures become more regular and more oriented perpendicular to the polarization direction of the laser radiation. Fig. 3(c) show cross sections along

the x-axis (at $y = 10\mu$m) of the results in Fig. 4. The spatial periodicity Λ of the structures in Fig. 4(i) and Fig. 3(c, bottom) was found to be in the range $0.14\lambda \leq \Lambda \leq 0.17\lambda$, where $\lambda = 800$nm is the wavelength of the laser radiation. This range of periodicities is within the expected range of those of HSFLs in Table 1. The averaged peak-to-valley height of HSFLs increases after each FDTD cycle. After 7, 8 and 9 FDTD cycles this height was found to equal about 150nm, 180nm and 205nm respectively, which are comparable to the values found by Hsu et al. (2008) on gallium phosphide. The orientation of the HSFLs in Fig. 4 is perpendicular to the polarization, which is not handled correctly by the analytical model of Sipe et al. Hence, the FDTD simulations including the simplified model of ablation, also are able to predict the formation and growth of HSFLs$_\perp$. The FDTD simulations including the simplified model of ablation was also found to predict HSFLs parallel to the polarization, but this result is not shown here.

4. Conclusions

The finite-difference time-domain (FDTD) method, to numerically solve the two coupled Maxwell's curl equations, for linear, isotropic, dispersive materials with no magnetic losses, was applied in order to simulate the interaction of laser radiation with the rough surface of a material. This simulation model was extended to include a simple non-physical model of laser material removal by ablation. Some simulation results in the space domain were presented and discussed. It was shown that the numerical FDTD model predicts several types of Laser-induced Periodic Surface Structures (LIPSSs), including Grooves, which are characterised by a spatial periodicity larger than the wavelength of the laser, as well as High Spatial Frequency LIPSSs (HSFLs) with an orientation perpendicular to the polarization of the laser radiation. Both types of LIPSSs are not handled correctly by the "classical" analytical Efficacy factor model. The FDTD model, and the FDTD model including a simple non-physical model of laser ablation, can explain LIPSS formation in the framework of an electromagnetic approach.

References

Anisimov, S.I., Inogamov, N.A. , Petrov, Y.V., Khokhlov, V.A., Zhakhovskii, V.V., Nishihara, K., Agranat, M.B., Ashitkov, S.I., Komarov, P.S., 2008. Interaction of short laser pulses with metals at moderate intensities Applied Physics A: Materials Science and Processing, 92(4), pp.939-943.

Baudach, S., Bonse, J., Kautek, W., 1999. Ablation experiments on polyimide with femtosecond laser pulses. Applied Physics A, 69,pp.395398.

Birnbaum. M., 1965. Semiconductor surface damage produced by ruby lasers. Journal of Applied Physics, 36, pp.3688-3689.

Bonse, J., Baudach, S., Krüger, J., Kautek, W., Lenzner., M., 2002. Femtosecond laser ablation of silicon modification thresholds and morphology. Applied Physics A, 74, pp.19-25.

Bonse, J., Höhm, S., Rosenfeld, A., Krüger, J., 2013. Sub-100-nm laser-induced periodic surface structures upon irradiation of titanium by Ti:sapphire femtosecond laser pulses in air. Applied Physics A, 110, pp.547-551.

Bonse, J., Krüger, J., 2010. Pulse number dependence of laser-induced periodic surface structures for femtosecond laser irradiation of silicon. Journal of Applied Physics, 108, pp.03490315.

Bonse, J., Munz, M., Sturm, H., 2005. Structure formation on the surface of indium phosphide irradiated by femtosecond laser pulses. Journal of Applied Physics, 97, pp.01353819.

Bonse, J., Rosenfeld, A., Krüger, J., 2009. On the role of surface plasmon polaritons in the formation of laser-induced periodic surface structures upon irradiation of silicon by femtosecond-laser pulses. Journal of Applied Physics, 106, pp.10491015.

Bonse, J., Sturm, H., Schmidt, D., Kautek, W., 2000. Chemical, morphological and accumulation phenomena in ultrashort-pulse laser ablation of TiN in air. Applied Physics A, 71, pp.657-665.

Borowiec A., Haugen,H. K., 2003. Subwavelength ripple formation on the surfaces of compound semiconductors irradiated with femtosecond laser pulses. Applied Physics Letters, 82, pp.44624464.

Breitling, D., Ruf, A., Dausinger, F., 2004. Fundamental aspects in machining of metals with short and ultrashort laser pulses. Proceedings of the SPIE, Vol. 5339, pp.49-63.

Csete, M., Hild, S., Plettl, A., Ziemann, P., Bor, Z., Marti, O., 2004. The role of original surface roughness in laser-induced periodic surface structure formation process on poly-carbonate films. Thin Solid Films, 453-454, pp.114-120.

Camacho-López, S., Camacho-López, M.A., Mejía, O. O., Evans, R., Vega, G.C., Camacho-López, M.A., Zaldivar, M.H., Garca, A.E., Bañuelos Muñetón, J.G., 2012. Processing of Metallic Thin Films Using Nd:YAG Laser Pulses, chap. 3, pp.2340, IntechOpen.

Costache, F., Kouteva-Arguirova, S., Reif, J., 2004. Sub-damage-threshold femtosecond laser ablation from crystalline Si: surface nanostructures and phase transformation, Applied Physics A, 79, pp.1429-1432.

Derrien, T.J., Krüger, J., Itina, T. E., Höhm, S., Rosenfeld, A., Bonse, J., 2013. Rippled area formed by surface plasmon polaritons upon femtosecond laser double-puls irradiation of silicon, Optics Express, 21(24), pp.29643-29655.

van Driel, H. M., Sipe, J. E., and Young, J. F., 1982. Laser-induced periodic surface structure on solids: A universal phenomenon. Physical Review Letters, 49(26), pp.1955-1958.

Emmony, D.C., Howson, R. P., Willis, L. J., 1973. Laser mirror damage in germanium at 10.6μm. Applied Physics Letters, 23, pp.598600.

Haneman, D., Nemanich, R.J., 1962. Surface topography of laser annealed silicon, Solid State Communications, 43, pp.203-206.

Höhm, S., Herzlieb, M., Rosenfeld, A., Krüger, Bonse, J., 2013. Formation of laser-induced periodic surface structures on fused silica upon two-color double-pulse irradiation, Applied Physics Letters, 103, pp.254101.

A. J. Huis in 't Veld and J. van der Veer. Initiation of femtosecond laser machined ripples in steel observed by scanning helium ion microscopy (SHIM). Journal of Laser Micro/Nanoengineering, 5, pp.28-34.

Hsu, E. M., Crawford, T. H. R., Maunders, C., Botton, G. A., and Haugen, H. K., 2008. Cross-sectional study of periodic surface structures on gallium phosphide induced by ultrashort laser pulse irradiation. Applied Physics Letters, 92, pp.221112.

Huang, M., Zhao, F., Cheng, Y., Xu, N., and Xu, Z., 2010. The morphological and optical characteristics of femtosecond laser-induced large-area micro/nanostructures on GaAs, Si, and brass. Optics Express, 18, pp.A600A619.

Jee,Y., Becker, M.F., Walser, R.M., 1988. Laser-induced damage on single-crystal metal surfaces. Journal of the Optical Society of America B, 5:648659, 1988.

Keilmann, F., Bai, Y.H., 1982. Periodic surface structures frozen into CO_2 lasermelted quartz. Applied Physics A, 29, pp.9-18.

Leveugle, E., Ivanov, D.S., Zhigilei, L.V., 2004. Photomechanical spallation of molecular and metal targets: Molecular dynamics study. Applied Physics A: Materials Science and Processing, 79(7), pp.16431655.

Lewis, L.S., Perez, D., 2009. Laser ablation with short and ultrashort laser pulses: Basic mechanisms from molecular-dynamics simulations. Applied Surface Science, 255(10), pp.5101-5106.

Lorazo, P., Lewis, L.J., Meunier, M., 2006. Thermodynamic pathways to melting, ablation, and solidification in absorbing solids under pulsed laser irradiation. Physical Review B, 73(13), pp.134108.

Oboňa, J.V., Skolski, J.Z.P., Römer, G.R.B.E., Huis in 't Veld, A.J., 2014. Pulse-analysis-pulse investigation of femtosecond laser-induced periodic surface structures on silicon in air. Optics Express.

Okada, T., Kawahara, H., Ishida, Y., Kumai, R., Tomita, T., Matsuo, S., Hashimoto, S., Kawamoto, M., Makita, Y., and Yamaguchi, M., 2008. Cross-sectional TEM analysis of laser-induced ripple structures on the 4H-SiC single-crystal surface. Applied Physics A, 92(3), pp.665668.

Perez, D. Lewis, L.J., 2003. Molecular-dynamics study of ablation of solids under femtosecond laser pulses. Physical Review B, 67(18), pp.184102.

Rethfeld, B., Sokolowski-Tinten, K., Anisimov, S., 2004. Timescales in the response of materials to femtosecond laser excitation. Applied Physics A, 79, pp. 767.

Römer, G.R.B.E., Skolski, J.Z.P., Vincenc Oboňa, J., Ocelík, V., de Hosson, J.Th.M., Huis in 't Veld, A.J., 2014. Laser-induced periodic surface structures, modeling, experiments and applications. Proc. of SPIE, Vol. 8968, pp.89680D-1-10.

Römer, G.R.B.E., Huis in 't Veld, A.J., Meijer, J., Groenendijk, M.N., 2009. On the formation of laser induced selforganizing nanostructures. CIRP Annals - Manufacturing Technology, 58(58), pp. 201204.

Siegrist, M., Kaech, G., Kneubühl, F., 1973. Formation of a periodic wave structure on the dry surface of a solid by TEA-CO_2-laser pulses. Applied Physics A, 2, pp.4546.

Sipe, J. E., Young, J. F., Preston, J. S., and van Driel, H. M., 1983. Laser-induced periodic surface structure. I. theory. Physical Review B, 27(2), pp.11411154.

Skolski, J.Z.P., Römer, G.R B.E., Oboňa, J.V., Ocelík, V., Huis in't Veld, A.J., De Hosson, J.Th.M., 2012. Laser-induced periodic surface structures: Fingerprints of light localization. Physical review B, 85, pp.075320.

Skolski, J.Z.P., Römer, G.R.B.E., Oboňa, J.V., Huis in 't Veld, A.J., 2014. Modeling laser-induced periodic surface structures: Finite-difference time-domain feedback simulations. Jorunal of Applied Physics, 115, pp.103102.

Skolski, J., 2014. Modeling of laser-induced periodic surface structures - an electromagnetic approach. PhD thesis, University of Twente, Enschede, The Netherlands (2014).

Skolski, J.Z.P., Römer, G.R.B.E., Oboňa, J.V., Ocelík, V., Huis in 't Veld, A.J., De Hosson, J.Th.M., 2013. Inhomogeneous absorption of laser radiation: Trigger of LIPSS formation. Journal of Laser Micro/Nanoengineering, 8(1), pp.15.

Temple, P., Soileau, M., 1981. Polarization charge model for laser-induced ripple patterns in dielectric materials. IEEE Journal of Quantum Electronics, 17, pp.2067- 2072.

Vorobyev, A. Y., Makin, V. S., Guo, C., 2007. Periodic ordering of random surface nanostructures induced by femtosecond laser pulses on metals. Journal of Applied Physics, 101, pp.03490314.

Wu, Q., Ma, Y., Fang, R., Liao, Y., Yu, Q., Chen, X., Wang, K., 2003. Femtosecond laser-induced periodic surface structure on diamond film. Applied Physics Letters, 82, pp.1703-1705.

Yasumaru, N., Miyazaki, K., Kiuchi, J., 2003. femmtosecond-laser-induced nanostructure formed on hard thin films of TiN and DLC. Applied Physics A, 76, pp.983-985.

Yee, K.S., 1966. Numerical solution of initial boundary value problems involving maxwells equations in isotropic media. IEEE Transactions on Antennas and Propagation. 14(3), pp.302-07.

Young, J. F., Preston, J. S., van Driel, H. M., Sipe, J. E., 1983. Laser-induced periodic surface structure. II. Experiments on Ge, Si, Al, and brass. Physical Review B, 27, pp.11551172.

Zhigilei, L.V., Lin, Z., Ivanov, D.S., 2009. Atomistic modeling of short pulse laser ablation of metals: Connections between melting, spallation, and phase explosion. The Journal of Physical Chemistry C, 113(27), pp.11892-11906.